J Biomol NMR (2007) 38:125–131
DOI 10.1007/s10858-007-9153-y

ARTICLE

Generation and relaxation of high rank coherences in AX_3 systems in a selectively methionine labelled SH2 domain

Karin Kloiber · Michael Fischer · Karin Ledolter · Michael Nagl · Walther Schmid · Robert Konrat

Received: 24 October 2006 / Accepted: 15 March 2007 / Published online: 9 May 2007
© Springer Science+Business Media B.V. 2007

Abstract The usefulness of selective isotope labelling patterns is demonstrated using the C-terminal SH2 domain of PLC-γ1 selectively ^{13}C labelled at methionine methyl groups. We demonstrate the generation and relaxation of coherences that are second rank in protons and first rank in carbons that derive from quadrupolar order in protons. The decay rates of second rank double quantum proton coherences are measured. These terms exhibit fewer channels for cross-correlated relaxation compared to single quantum coherences. Our results indicate the potential application of the measurement of high order proton coherences to the analysis of dynamics in methyl-bearing side chains.

Keywords Selective labelling · Methyl groups · Multipolar spin terms · Nuclear spin relaxation

Introduction

NMR spectroscopy presents a powerful probe of structural and dynamic properties of biomolecules on an atomic level. As such, it has been providing increasingly detailed information on thermodynamics and function of proteins. Traditionally, proteins are prepared by bacterial growth using minimal media supplemented with $^{15}NH_4Cl$ (and ^{13}C glucose) for recombinant protein synthesis, an approach that yields uniform incorporation of ^{15}N (and ^{13}C) spin labels. Although generally a high level of incorporation of NMR active nuclei is desired, in high molecular weight proteins spectral complexity can impede analysis of protein structure and dynamics. In addition, fast transverse relaxation in large proteins will exert an increasingly detrimental effect on the sensitivity of NMR experiments. In order to obtain more favourable relaxation properties, bacterial growth can be carried out in ^2H_2O, leading to high levels of deuteration at non-exchangeable positions. The gyromagnetic ratio of ^2H being about one sixth of that of ^1H, replacement of protons by deuterium efficiently reduces dipolar relaxation of nuclei that are otherwise directly attached or in close proximity to protons. Recently, techniques have become available that select slowly relaxing components of magnetization (Pervushin et al. 1997; Tugarinov et al. 2003) and thus push the size limit of structure determination to about 80 kDa, using per-deuterated molecules.

A complementary strategy to address experimental limitations concerning the analysis of large proteins aims at introducing NMR active (or inactive) labels at specific sites of the protein by supplementing growth media with selectively labelled amino acid precursors. Such an approach has been employed to reintroduce proton resonances in methyl groups for the collection of long-range distance information in otherwise deuterated molecules (Gardner et al. 1997), thereby maintaining the favourable relaxation properties of per-deuterated molecules and at the same time reducing spectral overlap. Site-specific labelling techniques often confer magnetic isolation of small spin systems, which is particularly desirable in certain spin relaxation measurements that serve to characterize local protein dynamics. Here, selective labelling facilitates the design of pulse

K. Kloiber (✉) · K. Ledolter · R. Konrat
Department of Biomolecular Structural Chemistry, Max F. Perutz Laboratories, University of Vienna, Campus Vienna Biocenter 5, Vienna 1030, Austria
e-mail: karin.kloiber@univie.ac.at

M. Fischer
e-mail: robert.konrat@univie.ac.at

M. Fischer · M. Nagl · W. Schmid
Institute of Organic Chemistry, University of Vienna, Währingerstrasse 38, Vienna 1090, Austria

sequences that would otherwise suffer from the complexity of the multiple interactions in an extended network of NMR active nuclei. Although some relaxation methods for methyl groups, for instance, work for uniformly ^{13}C labelled proteins or selectively labelled proteins with a certain degree of scrambling of carbon labels (Yamazaki et al. 1994; Millet et al. 2002; Mulder and Akke 2003), experiments that rely on selective labelling schemes are generally more sensitive, since in a system of two or more scalar coupled ^{13}C spins pulse sequence design is constricted by the need to prevent the undesired loss of magnetization due to the large one-bond carbon-carbon couplings. In addition, small scalar couplings across two or three bonds may cause significant systematic errors in certain types of relaxation experiments (CPMG or $R_{1\rho}$) if two nuclei cannot be manipulated separately (Mulder and Akke 2003; Ishima et al. 2004). Furthermore, for a carbon nucleus, the proximity of another ^{13}C label serves as an efficient dipolar relaxation channel and complicates the analysis of relaxation rates (Yamazaki et al. 1994; Ishima et al. 2001).

Methyl groups present extremely valuable probes of protein dynamics since they are mostly located in the hydrophobic cores of proteins and are involved in tertiary contacts that are crucial for protein fold and stability. In addition, resonances in methyl spectra are usually well-dispersed and intense due to fast methyl rotation. Here, we present novel methyl relaxation experiments using a selectively methionine methyl ^{13}C-labelled sample of the C-terminal SH2 domain of the signal transduction protein PLC–γ1 (PLCC SH2). We used these selective methyl labels to design a suite of 1D experiments by which we illustrate the generation of spherical tensor operators of second rank in the X_3 manifold of the AX_3 spin system. On the basis of the phase cycling strategies that are used in these 1D experiments to separate the desired terms, we propose two-dimensional pulse schemes to measure relaxation rates of coherences derived from quadrupolar order of protons, $T^H_{20}T^C_{1i}$, where i is equal to 0 or ±1. The strategy is similar to the one described in the context of deuterium relaxation in CH_2D isotopomers of methyl groups (Muhandiram et al. 1995; Millet et al. 2002).

Due to rapid rotation of the methyl group around a threefold symmetry axis, the X_3 system is conveniently represented by a sum of one totally symmetric manifold with group spin I = 3/2 and two asymmetric manifolds with group spin I = 1/2 (Muller et al. 1987; Kay et al. 1988; Kay et al. 1996); the AX_3 system accordingly consists in a convolution of these manifolds with another spin I = 1/2 system representing the carbon nucleus. In our experiments we employ double quantum filters on protons. Spin terms that derive from the two I = 1/2 manifolds of the X_3 subsystem do therefore not contribute to the observations, and theoretical considerations and analysis can be restricted to a spin system represented by an I = 3/2 nucleus coupled to a spin I = 1/2 nucleus. A schematic representation of the high order spin terms used in this work is given in Fig.1. For the description of the pulse sequences we adopt the spherical tensor operator notation (Muller et al. 1987) for both proton and carbon magnetization, where $T^H_{lp}T^C_{lp'}$ denotes operators of ranks l,l' and coherence orders p,p' in protons and carbon, respectively, as indicated by the superscript. Since for protons we need not consider the asymmetric I = 1/2 manifolds, we omit the indices referring to the group spin quantum number for the sake of simplicity.

Results

Figure 2 shows pulse sequences devised for the measurement of relaxation properties of the multipolar spin terms $T^H_{2\pm1}T^C_{10}$, $T^H_{2\pm2}T^C_{10}$ and $T^H_{2\pm2}T^C_{1\pm1}$. Panel a depicts the pulse

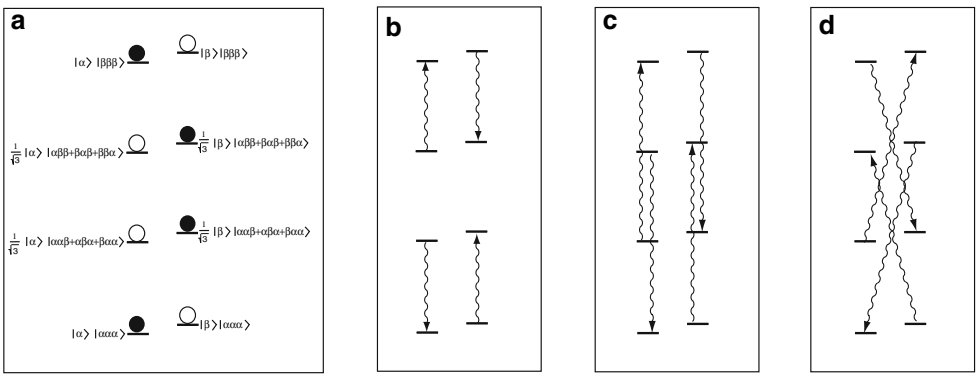

Fig. 1 Energy level diagrams for the spin I = 3/2 manifold of the AX_3 system. Depicted from left to right are (**a**) $T^H_{20}T^C_{10}$, (**b**)$T^H_{2\pm1}T^C_{10}$, (**c**) $T^H_{2\pm2}T^C_{10}$, and (**d**) $T^H_{2\pm2}T^C_{1\pm1}$. For $T^H_{20}T^C_{10}$, filled circles symbolize positive values for population, empty circles are depleted states. Coherences are depicted by wavy lines. Carbon and proton spin states that constitute the symmetrised basis are given for $T^H_{20}T^C_{10}$

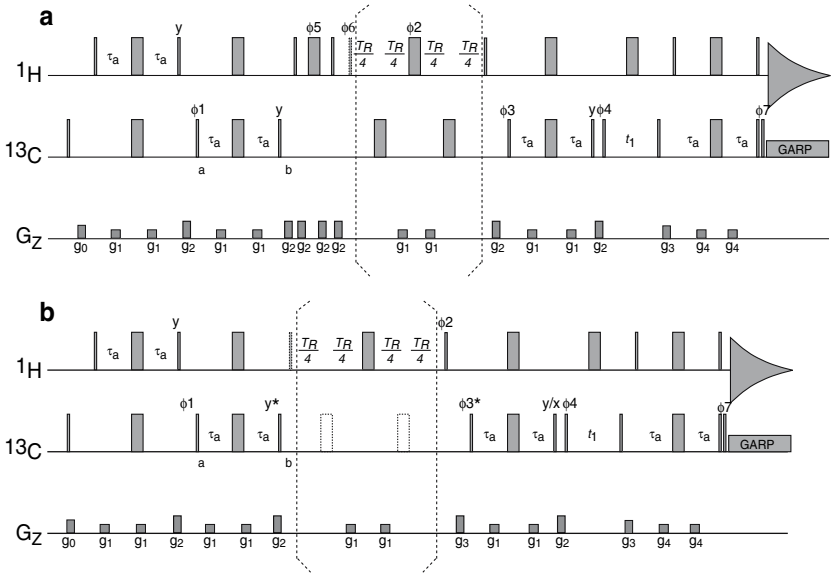

Fig. 2 Pulse schemes for the measurements of relaxation rates of $T^H_{2\pm1}T^C_{10}$, $T^H_{2\pm2}T^C_{10}$, and $T^H_{2\pm2}T^C_{1\pm1}$. Narrow and wide pulses indicate 90° and 180° pulses, respectively. All pulses are applied along the x-axis unless indicated otherwise. ^{1}H and ^{13}C pulses are centered at 4.77 and 17 ppm, respectively, the ^{1}H carrier frequency is shifted to 1.85 ppm during relaxation periods. ^{13}C decoupling is achieved using the GARP sequence (Shaka et al. 1985) with a 2.3 kHz field. Gradient levels were as follows: g_0 = 2 ms, 2 Gcm^{-1}, g_1 = 0.5 ms, 2 Gcm^{-1}, g_2 = 3 ms, 15 Gcm^{-1}, g_3 = 1 ms, –5 Gcm^{-1}, g_4 = 0.5 ms, 4 Gcm^{-1}. Quadrature detection in F1 is achieved via States-TPPI of ϕ_4. (**A**) Pulse scheme for the measurement of the decay of $T^H_{2\pm1}T^C_{10}$. Double quantum filtering is achieved by the means of cycling ϕ_5 in steps of 45° whereas the receiver is cycled by 180°. The hatched pulse is applied with a flip angle of 45° in order to generate the maximum amount of single quantum coherence. Phase cycling is ϕ_1 = x, –x, ϕ_2 = 2(x), 2(-x), ϕ_3 = 2(x) 2(-x), ϕ_4 = x, ϕ_5 = 2(0°), 2(90°), 2(45°), 2(135°), ϕ_6 = 4(x), 4(–x), rec = x, –x, –x, x, –x, x, x, –x. (**B**) Pulse sequence for the measurement of the relaxation of $T^H_{2\pm2}T^C_{10}$ and $T^H_{2\pm2}T^C_{1\pm1}$. Here, the double quantum filter is incorporated into the relaxation delay and the hatched pulse is applied with a 90° flip angle. Pulses with an asterisk are applied with the purpose of generating $T^H_{2\pm2}T^C_{10}$, but are omitted for measuring relaxation of $T^H_{2\pm2}T^C_{1\pm1}$. Dotted 180° pulses during relaxation need not be applied in case carbon is longitudinal. The phase of the pulse following the first INEPT step during back transfer has phase y (x) for $T^H_{2\pm2}T^C_{10}$($T^H_{2\pm2}T^C_{1\pm1}$). Phase cycling is ϕ_1 = x, –x, ϕ_2 = 4(x), 4(y), ϕ_3 = 2(x), 2(–x), ϕ_4 = x, rec = x, –x, –x, x, –x, x, x, –x

scheme used for measuring the decay of $T^H_{2\pm1}T^C_{10}$. Magnetization starts from any of the three methyl protons and is transferred to the attached carbon nucleus via an INEPT step. At point ***a*** in the sequence the magnetization of interest is $T^H_{10}T^C_{1\pm1}$. It evolves due to $^1J_{CH}$ for a delay $1/(2^1J_{CH})$ and is transformed into $T^H_{20}T^C_{10}$ (quadrupolar order of protons) at point ***b***. A proton double quantum filter is employed to exclude terms that are not derived from this second rank term. It consists in a 90°–180°–90° pulse element on proton magnetization where the 180° pulse is cycled in steps of 45° and the receiver is cycled in steps of 180° in order to select a change in proton coherence order $\Delta p^H = \pm4$. Alternatively, either of the two 90° pulses can be cycled by 90° to select $\Delta p^H = \pm2$; either way, double quantum coherence of protons is selected (Millet et al. 2002), whereas terms arising from the asymmetric proton manifolds are suppressed (the phase cycle is given explicitly in the caption of Fig. 2). The second 90° pulse restores $T^H_{20}T^C_{10}$, and $T^H_{2\pm1}T^C_{10}$ is created by a 45° pulse. $\Delta p^H = \pm1$ is selected by simultaneously shifting the phase of ϕ_6 and the receiver. After the relaxation delay, T_R, transfer of magnetization is reversed and carbon magnetization is allowed to evolve during t_1. Magnetization is subsequently transferred back to the methyl protons, yielding a 2-dimensional ^{13}C–^{1}H correlation map where intensities are modulated during the relaxation period. In panel b, a similar pulse sequence is depicted for the measurement of the decay of $T^H_{2\pm2}T^C_{10}$ and $T^H_{2\pm2}T^C_{1\pm1}$. The sequence is identical to the first one until point ***b***. The relaxation delay is subsequently implemented with the double quantum filter incorporated, and the desired coherence is excited using a 90° proton pulse. No additional phase cycling is necessary. The carbon pulses indicated by asterisks serve to generate $T^H_{2\pm2}T^C_{10}$ during the relaxation period and are omitted if the $T^H_{2\pm2}T^C_{1\pm1}$ is monitored.

The generation of multipolar proton spin terms from $T^H_{20}T^C_{10}$ as a function of proton pulse length was monitored using 1D versions of these pulse sequences. In addition, $T^H_{20}T^C_{10}$ was selected by applying a pulsed field gradient after the excitation pulse. The experimental dependence of the intensities of the coherences generated from quadrupolar order on the proton pulse length is depicted in Fig. 3, where circles correspond to the normalized intensities of

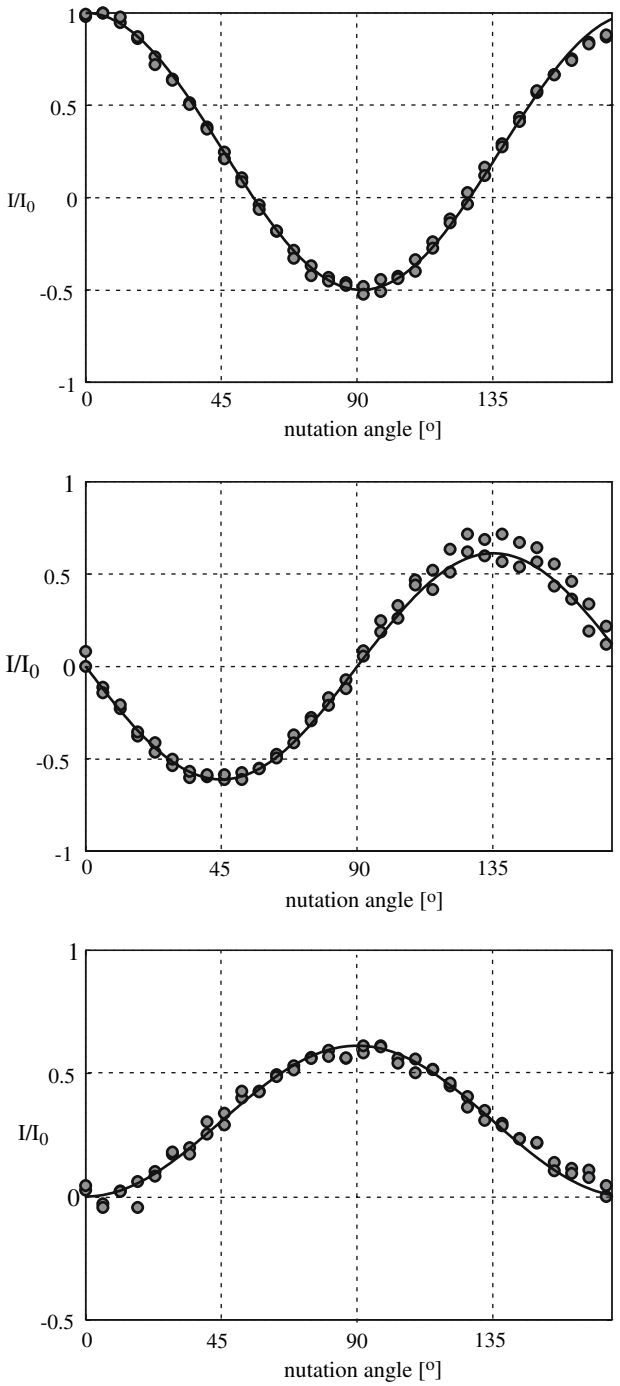

Fig. 3 Amount of magnetization as a function of proton flip angle: (**a**) $T^H_{20}T^C_{10}$, (**b**) $T^H_{2\pm1}T^C_{10}$, (**c**) $T^H_{2\pm2}T^C_{10}$. The two most intense peaks were chosen from a 1D experiment. The flip angle has been determined to give the best fit for the two resonances and three spin terms simultaneously. Normalization was with respect to the first data point in each series. The theoretical dependence is given by reduced Wigner matrix elements $d^2_{00} = 1/2(3\cos^2\beta - 1)$, $d^2_{\pm10} = \sqrt{3/2}\sin\beta\cos\beta$, and $d^2_{\pm20} = \sqrt{3/8}\sin^2\beta$ where β is the proton flip angle of the pulse applied to $T^H_{20}T^C_{10}$

the two strongest resonances that were resolved in the 1D spectra. The effect of applying pulses of flip angle β is described by reduced Wigner matrix elements, $T^H_{2p}T^C_{10} = d^2_{p0}(\beta)e^{-i(p-2)\varphi}$, where $\varphi = 0$ indicates a y-pulse (Muller et al. 1987). Experimental results are in excellent agreement with theory. Complete destruction of $T^H_{20}T^C_{10}$ occurs at the magic angle, whereas flip angles for maximum excitation of $T^H_{2\pm1}T^C_{10}$ and $T^H_{2\pm2}T^C_{10}$ are 45° and 90°, respectively. Figure 3 demonstrates that it is not possible by the mere application of pulses to separate $T^H_{2\pm1}T^C_{10}$ or $T^H_{2\pm2}T^C_{10}$ from quadrupolar order. Separation is instead accomplished by appropriate phase cycling as described above.

Decays of $T^H_{2\pm2}T^C_{10}$ and $T^H_{2\pm2}T^C_{1\pm1}$ of the four methionine methyl groups are depicted in Fig. 4. Rates are generally high and differ strongly for the four resonances, indicating that the relaxation properties of these coherences respond very strongly to differences in motion and/or differences in proton density of their respective surrounding. $T^H_{2\pm2}T^C_{10}$ relaxes slightly faster than $T^H_{2\pm2}T^C_{1\pm1}$. Experimental relaxation rates are given in Table 1. If suppression of ^{1}H-^{13}C/^{1}H-^{1}H dipolar cross-correlated relaxation is desired, it is recommended to apply a train of 180° pulses on carbon during the relaxation periods at a rate that is fast compared to the cross-correlation rate. Notably, we did not observe significant deviations from mono-exponentiality in any of the relaxation decays we recorded, although pulse trains on carbon were not applied. However, two carbon 180° pulses are applied after delays of $T_R/4$ and $3T_R/4$, such that the maximum evolution period before inversion of ^{1}H-^{13}C/^{1}H-^{1}H dipolar cross-correlated relaxation was 12.5 ms. Furthermore, loss of correlation can be caused by rapid spin flips of the dipolar coupled methyl proton due to the contribution of non-bonded protons to proton longitudinal relaxation (Ishima et al. 2001; Tugarinov and Kay 2004), thereby suppressing cross-correlated relaxation pathways in the protonated background of our sample. Of note, $T^H_{2\pm2}T^C_{1\pm1}$ is even less affected by dipolar cross-correlated relaxation. A detailed investigation of the effects of cross-correlated relaxation will be published elsewhere.

Summary

We have used uniformly ^{15}N labelled and selectively methionine methyl ^{13}C–labelled PLCC SH2 in order to demonstrate the potential use of high rank methyl proton spin terms in NMR relaxation spectroscopy. The strategy of precursor synthesis follows the one that was described recently (Lichtenecker et al. 2004). Details of the precursor synthesis and its selective incorporation into the protein are described elsewhere (Fischer et al. 2007).

The generation of multipolar proton spin terms was monitored as a function of pulse length in order to devise the phase cycling procedures that are necessary to monitor the relaxation properties of proton second rank

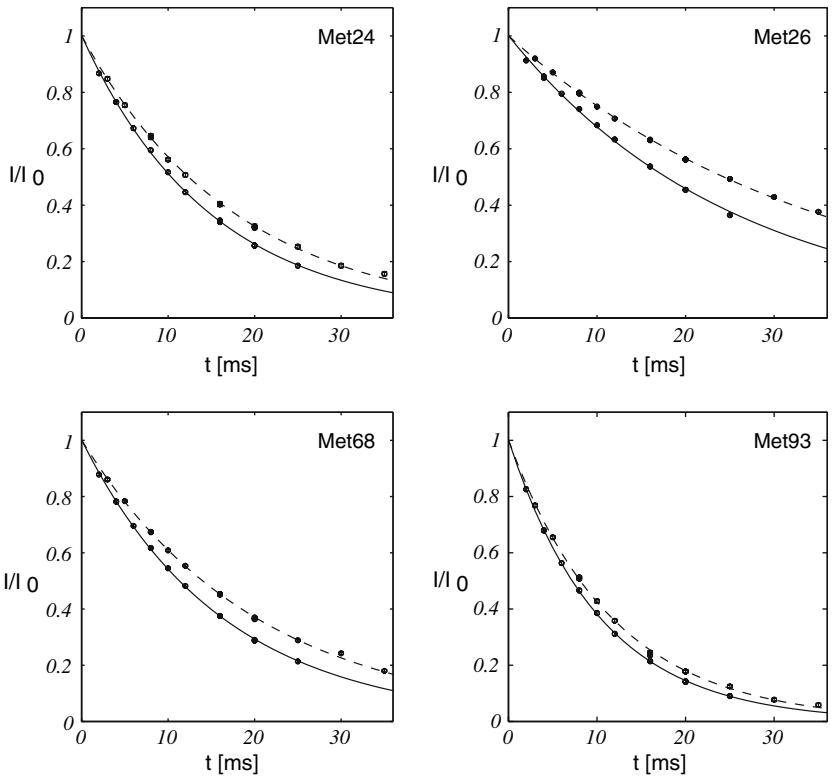

Fig. 4 Multiple quantum decays of $T^H_{2\pm2}T^C_{10}$ (solid line), $T^H_{2\pm2}T^C_{1\pm1}$ and (dashed line) of the four Methionine peaks in the C-terminal SH2 domain of PLC-γ1. Intensities have been normalized to 1 and error estimates are based on MC analysis using the noise level as a measure for random uncertainty (error bars are smaller than the symbol size)

Table 1 Relaxation rates of the methyl groups of the four methionine residues in the carboxyl-terminal SH2 domain of PLCC-γ1 at 18.8T. Assignments were taken from the BMRB, entry 5310 (Kay et al. 1996)

	$R(T^H_{20}T^C_{1\pm1})[s^{-1}]$	$R(T^H_{20}T^C_{10})[s^{-1}]$
M24	56.2 ± 0.8	67.0 ± 1.0
M26	28.6 ± 0.3	39.0 ± 0.4
M68	49.5 ± 0.4	61.4 ± 0.6
M93	85.8 ± 1.4	96.2 ± 1.4

coherences in methyl groups. Exemplary decays of the coherences $T^H_{2\pm2}T^C_{10}$ and $T^H_{2\pm2}T^C_{1\pm1}$ demonstrate the excellent sensitivity despite of the fast relaxation of the coherences. Although in methionine residues the flow of magnetization is not compromised by one-bond ^{13}C–^{13}C scalar couplings, the isolation of the ^{13}C spin in methionine groups may nonetheless be crucial in CPMG or $R_{1\rho}$ experiments because artefacts are introduced by small scalar couplings to more remote carbon nuclei (Mulder and Akke 2003; Ishima et al. 2004).

To date, methyl dynamics have been studied mainly by ^{13}C and ^{2}H NMR relaxation techniques since the relaxation properties of these nuclei are hardly sensitive to the presence of external protons (Ishima et al. 2001). Qualitative correlation between proton transverse relaxation in CHD_2 groups and ^{13}C (^{2}H) transverse relaxation rates in CHD_2 (CH_2D) methyl isotopomers has been reported (Ishima et al. 2001) for HIV-1 protease. Only recently, the potential role of proton relaxation in the analysis of methyl group dynamics has been demonstrated for the 7.5 kDa protein L and the 82 kDa protein MSG (Tugarinov and Kay 2006) with selectively ^{13}C–^{1}H labelled methyl groups of Val, Leu, and Ile. Both these approaches employ single quantum coherences of protons. Here we present another approach to qualitatively address methyl dynamics, using second rank double quantum coherences. The advantage of these spin terms lies in the reduction of cross-correlated relaxation channels as compared to single quantum terms. Generally, the number of cross-correlated relaxation pathways decreases with the number of nuclei involved in the coherence. As such, $T^H_{3\pm3}T^C_{1\pm1}$ is the term that is entirely devoid of intra-methyl cross-correlated relaxation. Generation of third rank terms is possible (Skrynnikov et al. 2001), their systematic investigation is, however, beyond the scope of this work and will be addressed in future studies. With our approach we find relaxation rates between 28 and 85 s^{-1} ($T^H_{2\pm2}T^C_{1\pm1}$), and 39 and 97 s^{-1} ($T^H_{2\pm2}T^C_{10}$), respectively, for the methionine methyl groups in PLCC SH2. Relaxation is systematically slightly faster for $T^H_{2\pm2}T^C_{10}$ due to additional contributions from C–H dipolar interactions. Notably, relaxation rates are highest for Met93, for which an order parameter has been reported that is significantly higher than for the other methionines (Kay et al. 1996). This qualitative agreement demonstrates

the potential applicability of the proton relaxation measurements for the analysis of methyl group dynamics. For a more rigorous interpretation of rates in terms of dynamics it will be necessary to perform experiments in a completely deuterated background.

Materials and methods

Protein preparation and purification

E. coli BL21(DE3) containing the expression plasmid for PLCC SH2 were grown in minimal media supplemented with $^{15}NH_4Cl$ and ^{12}C–glucose. Precursor (keto-methiobutyrate) was added to the growth medium prior to induction with IPTG. The protein was purified to homogeneity by affinity chromatography on a phosphocellulose column and subsequent size exclusion chromatography. The NMR sample (^1H,^{15}N, methionine-$^{13}CH_3$ PLCC SH2) was 1 mM in protein, 20 mM potassium phosphate, at pH 6.5 and contained 8% ^2H_2O.

NMR spectroscopy

Measurements were performed at 25 °C on Varian *Inova* Spectrometers operating at static magnetic field strengths of 11.8 and 18.8T. Experiments devised for the generation of quadrupolar order $T^H_{20}T^C_{10}$, and coherences $T^H_{2\pm1}T^C_{10}$ and $T^H_{2\pm2}T^C_{10}$ were recorded at 11.8 T in a 1D manner by arraying the length of the proton pulse that generates the desired coherences from $T^H_{20}T^C_{10}$ between 0 and 18 μ s in steps of 0.6 μ s, which covered nutation angles between 0 and 180°. Relaxation experiments for $T^H_{2\pm2}T^C_{10}$ and $T^H_{2\pm2}T^C_{1\pm1}$ were recorded at 18.8 T. Spectra had (224 × 1630) and (184 × 1630) complex data points for $T^H_{2\pm2}T^C_{10}$ and $T^H_{2\pm2}T^C_{1\pm1}$, respectively. Relaxation delays were (2, 4, 4, 6, 8, 10, 12, 16, 16, 20, 20, 25) ms for $T^H_{2\pm2}T^C_{10}$ and (3, 5, 8, 8, 10, 12, 16, 16, 20, 20, 25, 30, 35) ms for $T^H_{2\pm2}T^C_{1\pm1}$.

Data analysis

Spectra were processed using the nmrPipe Software package (Delaglio et al. 1995). The generation of the desired spin terms was followed by measuring peak heights of two of four non-overlapping proton resonances in a suite of 1D spectra using VNMR software. Curves in Fig. 2 were obtained by a simultaneous fit of the theoretical relationship between flip angle and amount of $T^H_{20}T^C_{10}$, $T^H_{2\pm1}T^C_{10}$, and $T^H_{2\pm2}T^C_{10}$ to the respective measured signal intensities, and of the 2 × 3 data sets using in-house written software (Matlab, The MathWorks Incs., USA). For relaxation experiments, partial peak volumes were determined via summation over a grid of 7 × 7 data points distributed around the centre of each peak position. Analysis of data was accomplished using in-house written software (Matlab, The MathWorks Incs., USA). For the computation of relaxation rates, a mono-exponential decay was fitted to the data. Error estimation is based on a Monte Carlo analysis (100 steps) where peak intensities were varied according to a normal distribution with a width calculated on the basis of the estimated noise level. Errors in experimental intensities (Fig. 4) correspond to standard deviations of the randomised intensities, and errors in rates are given as standard deviation of extracted rates (Table 1).

Acknowledgements We are grateful to Prof. Julie D. Forman-Kay for kindly providing the expression plasmid for PLCC (SH2). Funding was provided by the Austrian Science Foundation (F17) and the WWTF (LS162). R.K. thanks the FWF for start-up funding. K.K. is a recipient of an APART-fellowship of the Austrian Academy of Sciences at the Institute of Biomolecular Structural Chemistry, Vienna.

References

Delaglio F, Grzesiek S, Vuister GW, Zhu G, Pfeifer J, Bax A (1995) NMRPipe: a multidimensional spectral processing system based on UNIX pipes. J Biomol NMR 6:277–293

Fischer M, Kloiber K, Haeusler J, Ledolter K, Konrat R, Schmid W (2007) Synthesis of a ^{13}C-Methyl-group-labeled methionine precursor as a useful tool for simplifying protein structural analysis by NMR spectroscopy. Chem Bio Chem 8:610-612

Gardner KH, Rosen MK, Kay LE (1997) Global folds of highly deuterated, methyl-protonated proteins by multidimensional NMR. Biochemistry 36:1389–1401

Ishima R, Baber J, Louis JM, Torchia DA (2004) Carbonyl carbon transverse relaxation dispersion measurements and ms-micros timescale motion in a protein hydrogen bond network. J Biomol NMR 29:187–198

Ishima R, Petkova AP, Louis JM, Torchia DA (2001) Comparison of methyl rotation axis order parameters derived from model-free analyses of $^{(2)}H$ and $^{(13)}C$ longitudinal and transverse relaxation rates measured in the same protein sample. J Am Chem Soc 123:6164–6171

Kay LE, Holak TA, Prestegard JH (1988) AX3 spin system dynamics from forbidden cross peaks in double-quantum two-dimensional NMR experiments, with application to Acyl carrier protein. J Magn Reson 76:30–40

Kay LE, Muhandiram DR, Farrow NA, Aubin Y, Forman-Kay JD (1996) Correlation between dynamics and high affinity binding in an SH2 domain interaction. Biochemistry 35:361–368

Lichtenecker R, Ludwiczek ML, Schmid W, Konrat R (2004) Simplification of protein NOESY spectra using bioorganic precursor synthesis and NMR spectral editing. J Am Chem Soc 126:5348–5349

Millet O, Muhandiram DR, Skrynnikov NR, Kay LE (2002) Deuterium spin probes of side-chain dynamics in proteins. 1. Measurement of five relaxation rates per deuteron in $^{(13)}C$-labeled and fractionally $^{(2)}H$-enriched proteins in solution. J Am Chem Soc 124:6439–6448

Muhandiram DR, Yamazaki T, Sykes BD, Kay LE (1995) Measurement of ^2H T1 and T1r relaxation times in uniformly ^{13}C-

Labeled and fractionally 2H-labeled proteins in solutions. J Am Chem Soc 117:11536–11544

Mulder FAA, Akke M (2003) Carbonyl ^{13}C transverse relaxation measurements to sample protein backbone dynamics. Magn Reson Chem 41:853–865

Muller N, Bodenhausen G, Ernst R (1987) Relaxation-induced violations of coherence transfer selection rules in nuclear magnetic resonance. J Magn Reson 75:297–334

Pervushin K, Riek R, Wider G, Wuthrich K (1997) Attenuated T2 relaxation by mutual cancellation of dipole-dipole coupling and chemical shift anisotropy indicates an avenue to NMR structures of very large biological macromolecules in solution. Proc Natl Acad Sci USA 94:12366–12371

Shaka AJ, Barker PB, Freeman R (1985) Computer-optimized decoupling scheme for wideband applications and low-level operation. J Magn Reson 64:547–552

Skrynnikov NR, Mulder FA, Hon B, Dahlquist FW, Kay LE (2001) Probing slow time scale dynamics at methyl-containing side chains in proteins by relaxation dispersion NMR measurements: application to methionine residues in a cavity mutant of T4 lysozyme. J Am Chem Soc 123:4556–4566

Tugarinov V, Kay LE (2004) Cross-correlated relaxation enhanced ^{1}H-^{13}C NMR spectroscopy of methyl groups in very high molecular weight proteins and protein complexes. J Biomol NMR 29:369–376

Tugarinov V, Kay LE (2006) ^{1}H,^{13}C-^{1}H,^{1}H dipolar cross-correlated spin relaxation in methyl groups. J Am Chem Soc 128:7299–7308

Tugarinov V, Hwang PM, Ollerenshaw JE, Kay LE (2003) Relaxation rates of degenerate ^{1}H transitions in methyl groups of proteins as reporters of side-chain dynamics. J Am Chem Soc 125:10420–10428

Yamazaki T, Muhandiram DR, Kay LE (1994) NMR Experiments for the measurement of carbon relaxation properties in highly enriched, uniformly ^{13}C,^{15}N-labeled Proteins: Application to ^{13}Ca Carbons. J Am Chem Soc 116:8226–8278